Wait-Hill MoM for a lumped element loaded mesh screen on a stratified substrate

Christos Mias, *Member, IEEE*, and Angelo Freni, *Senior Member, IEEE*

***Abstract*— The generalized thin-wire Wait-Hill method of moments formulation in free space is extended to model plane wave scattering from a lumped element periodically loaded mesh screen backed by a multi-layer substrate. It is numerically demonstrated that the sawtooth function methodology proposed by Hill and Wait for reducing the computation time is applicable. Furthermore, for the case of an electrically dense mesh, a simple analytical expression for the transmission coefficient is obtained.**

***Index Terms*— Electromagnetic scattering by periodic structures, wire grids**

I. Introduction

TAILORED electromagnetic and equivalent circuit methods for modeling periodic structures have several advantages as discussed in [1]. One such method is the thin-wire entire-domain basis function method of moments (MoM) formulation of D.A. Hill and J.R. Wait for modeling plane wave scattering from a perfectly electrically conducting unloaded mesh in free space [2]. To significantly reduce the computation time of the method, the authors of [2] proposed the use of a discontinuous periodic sawtooth function. Furthermore, K.F. Casey added loss to the unloaded wire mesh and a dielectric substrate layer and based on [2] derived, in the limit of an electrically dense mesh, simple analytical expressions for the equivalent circuit impedance and transmission coefficient of the structure that improve one's insight of the shielding behavior of unloaded wire-mesh screens [3][4]. Based on the free space formulation of [5], the MoM formulation of [2] was generalized to include periodic lumped element loading in the mesh in order to model and obtain insight into the behavior of lumped element loaded frequency selective surfaces (FSS) in free space [6]. The lumped elements may be of surface mount or printed form.

In this paper, the free-space formulation in [6] is extended to include a multi-layer substrate (Fig. 1). By comparison with the commercial software CST (which is based on a different computational method) it is shown that the sawtooth function methodology in [2] for reducing the computation time is still applicable.

Manuscript received March 12 2015.

C. Mias is with the School of Engineering, University of Warwick, Coventry, CV4 7AL, UK (e-mail: c.mias@warwick.ac.uk).

A. Freni is with the Department of Information Engineering, University of Florence, I-50139 Firenze, Italy.

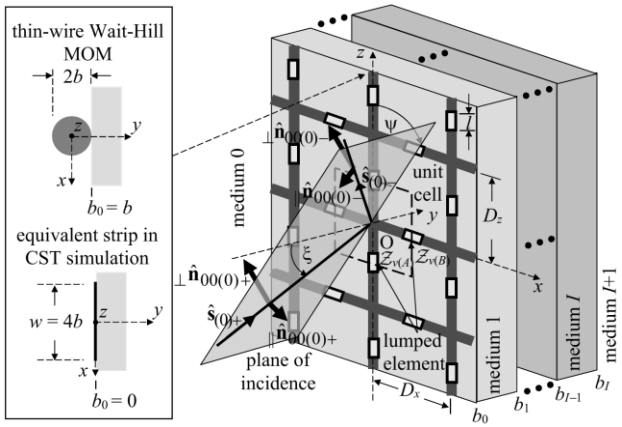

Fig. 1. Geometry of the lumped element periodically loaded mesh with a multilayer substrate.

By making use of the equivalent radius narrow strip approximation [7] (Fig. 1), a very good agreement between the results of the proposed thin-wire Wait-Hill MoM formulation and the narrow-strip CST results is demonstrated. In addition, for the case of an electrically dense mesh, a novel simple analytical expression for the transmission coefficient is obtained for the configuration in Fig. 1. Potential applications are FSS on building materials [8],[9] and FSS for the automotive industry [10] where multi-layer substrates can be present. Furthermore, the proposed formulations, due to their low computational requirements, can be used in novel fast ray-tracing software tools for designing frequency selective buildings through FSS [11]. Formulations for lumped element loaded FSS on multi-layer substrates were also proposed in [1], however they were restricted to vertical grids.

II. The Wait-Hill MoM formulation

The periodically loaded mesh configuration of the thin-wire Wait-Hill MoM is defined in Fig. 1. The mesh lies in medium 0 with constitutive parameters defined in Section II of [1]. The axes origin, reference unit cell coordinates and wire labelling are shown in Fig. 1 and are also defined in [6]. The electric field (**E**) boundary condition expression looks the same as that of (6) of [1], however it is applied here to both reference wires and includes the coupling between these wires,

$$\left({}_{\vartheta}\mathbf{E}^{inc} + {}_{\vartheta}\mathbf{E}^{ref\,(inc)} + \mathbf{E}^{sc} + \mathbf{E}^{ref\,(sc)} \right) \bullet \hat{\mathbf{u}} \Big|_{\mathbf{R}=\mathbf{R_b}} = \mathcal{Z}_{L(K)}(u) I_K(u) \tag{1}$$

$\hat{\mathbf{u}} = \hat{\mathbf{z}}$, $\mathbf{R}_b = \mathbf{R}_b(0,b,z)$ for wire *A* and $\hat{\mathbf{u}} = \hat{\mathbf{x}}$, $\mathbf{R}_b = \mathbf{R}_b(x,b,0)$ for wire *B*. The per unit length load impedance, $\mathcal{Z}_{L(K)}(u)$, of the

reference unit cell is defined in terms of the lumped element impedance $\mathcal{Z}_{\nu(K)}$ and Fourier series coefficients $Z_{n(K)}$ as shown in (5) and (6) of [6] where K=A, u=z for reference wire A and K=B, u=x for reference wire B. Multiple lumped elements can be included in the formulation by modifying $Z_{n(K)}$, see (1)-(4) of [5]. The current $I_K(u)$ is related to the unknown Fourier series current coefficients ${}_{\vartheta}A_m$ and ${}_{\vartheta}B_q$ as shown in (7) and (8) of [6]. The integers m and q denote the index of periodicity along the z-direction and x-direction respectively. It is assumed, for simplicity, that $b_0 = b$. In (1), the incident electric field, ${}_{\vartheta}\mathbf{E}^{inc}$, is given by (1) of [1] and ${}_{\vartheta}\mathbf{E}^{ref(inc)}$ is its reflection at the b_0 interface in the absence of the wires. The expression of ${}_{\vartheta}\mathbf{E}^{ref(inc)}$ is given by (8) of [1] multiplied by $\exp(-2jk_{r(0)}s_{y(0)}b)$. $\mathbf{E}^{sc}$ is the radiated field from the wires and $\mathbf{E}^{ref(sc)}$ is its reflection from the b_0 interface. The expression for $\mathbf{E}^{sc}$ is the same as that of (4) in [1] but without the Bessel term (as narrow strips are used in [1] whereas thin wires are used here), and for wire A is [12]

$$\mathbf{E}^{sc} = -\frac{\eta_{(0)}}{2D_x}\sum_{m=-\infty}^{\infty}\sum_{q=-\infty}^{\infty} {}_{\vartheta}A_m \frac{e^{-jk_{r(0)}\hat{\mathbf{r}}_{mq(0)\pm}\bullet\mathbf{R}}}{r_{mqy(0)}} \times \left({}_{\perp}n_{mqz(0)}\,{}_{\perp}\hat{\mathbf{n}}_{mq(0)\pm} + {}_{||}n_{mqz(0)}\,{}_{||}\hat{\mathbf{n}}_{mq(0)\pm}\right) \tag{2}$$

Equation (2) is obtained using the thin wire magnetic vector potential procedure described in [12]. The $\mathbf{E}^{ref(sc)}$ expression is the same as that of (9) in [1] (again without the Bessel term),

$$\mathbf{E}^{ref(sc)} = -\frac{\eta_{(0)}}{2D_x}\sum_{m=-\infty}^{\infty}\sum_{q=-\infty}^{\infty} {}_{\vartheta}A_m \frac{e^{-jk_{r(0)}\hat{\mathbf{r}}_{mq(0)-}\bullet\mathbf{R}}}{r_{mqy(0)}} \left({}_{\perp}\Re^{e}_{mq(0)+}\,{}_{\perp}n_{mqz(0)}\,{}_{\perp}\hat{\mathbf{n}}_{mq(0)-} + {}_{||}\Re^{e}_{mq(0)+}\,{}_{||}n_{mqz(0)}\,{}_{||}\hat{\mathbf{n}}_{mq(0)-}\right) e^{-2jk_{r(0)}s_{y(0)}b} \tag{3}$$

For wire B, $\mathbf{E}^{sc}$ and $\mathbf{E}^{ref(sc)}$ are obtained from (2) and (3), respectively, by substituting the subscript x with z (and vice-versa) and ${}_{\vartheta}A_m$ with ${}_{\vartheta}B_q$. The effective reflection coefficient ${}_{\perp,||}\Re^{e}_{mq(\chi)+}$ of the $(m,q)_{\text{th}}$ harmonic at the interface between media χ and χ+1 is defined in equation D.14 of [12]. The use of the effective reflection coefficient allows the multiple layers to be taken into account as described in [12]. Subscripts on the right include the harmonic order, "m and/or q", the Cartesian coordinate "x,y,z" for vector components, and the medium index which appears within round brackets. Polarization subscripts ($\perp$,$\|$) appear on the left of a variable. The direction vector of the mq_{th} harmonic is defined as $\hat{\mathbf{r}}_{mq(\chi)\pm} = r_{qx(\chi)}\hat{\mathbf{x}} \pm r_{mqy(\chi)}\hat{\mathbf{y}} + r_{mz(\chi)}\hat{\mathbf{z}}$ in medium χ and its components can be obtained from eqs. (4.24), (5.3)-(5.5) of [12]. ${}_{\|,\perp}n_{mqz(\chi)}$ is the z-component of the polarization unit vectors ${}_{\|,\perp}\hat{\mathbf{n}}_{mq(\chi)\pm}$ of the mq_{th} harmonic in medium χ which are defined in equations (4.55) and (4.56) of [12]. The subscripts $\pm$ on the right of variables refer to the harmonic direction vector above. As was done for the loaded wire grid in free space in [6], i.e. starting from (1), following the methodology of [2] and [5], and incorporating the discontinuous periodic sawtooth function (proposed in [2] to significantly reduce the computation time of the method), the following formulae are obtained

$$\hat{Z}_{m(A)}\,{}_{\vartheta}A'_m + \sum_{n=-\infty}^{\infty}{}'\, Z_{n(A)}\,{}_{\vartheta}A'_{m-n} - \sum_{q=-\infty}^{\infty} C^{(m)}_{q(B)}\,{}_{\vartheta}B'_q + U_m\Delta = \delta_{m0}\Phi^{inc} \tag{4}$$

$$-\sum_{m=-\infty}^{\infty} C^{(q)}_{m(A)}\,{}_{\vartheta}A'_m + \hat{Z}_{q(B)}\,{}_{\vartheta}B'_q + \sum_{n=-\infty}^{\infty}{}'\, Z_{n(B)}\,{}_{\vartheta}B'_{q-n} - V_q\Delta = \delta_{0q}\Psi^{inc} \tag{5}$$

where δ_{ij} is the Kronecker delta ($\delta_{ij} = 1$ for $i = j$ and $\delta_{ij} = 0$ for $i \neq j$). Equations (4) and (5) are similar to (24) and (25) in [6] however the various terms are different, because of the presence of the multiple layers, as follows

$${}_{\vartheta}\Phi^{inc} = \left(1 + {}_{\vartheta}\Re^{e}_{00(0)+}\right){}_{\vartheta}n_{00z(0)}\,E_0\,e^{-jk_{r(0)}s_{y(0)}b} \tag{6}$$

$$C^{(m)}_{q(B)} = \frac{j\omega\mu}{2D_z}\frac{e^{-\Gamma_{mq(0)}b}}{\Gamma_{mq(0)}} \times [r_{mz(0)}r_{qx(0)} - ({}_{\perp}n_{mqx(0)} \times {}_{\perp}n_{mqz(0)}\,{}_{\perp}\Re^{e}_{mq(0)+} + {}_{||}n_{mqx(0)}\,{}_{||}n_{mqz(0)}\,{}_{||}\Re^{e}_{mq(0)+})] \tag{7}$$

In medium χ, $\Gamma_{mq(\chi)} = jk_{r(\chi)}r_{mqy(\chi)}$. The expression for ${}_{\vartheta}\Psi^{inc}$ is obtained from the expression for ${}_{\vartheta}\Phi^{inc}$ by replacing in (6) ${}_{\vartheta}n_{00z(0)}$ with ${}_{\vartheta}n_{00x(0)}$. The expression for $C^{(q)}_{m(A)}$ is obtained from that of $C^{(m)}_{q(B)}$ by replacing in (7) D_z with D_x. It is to be noted that the aforementioned coupling terms C are due to the coupling between the orthogonal wires and hence do not appear in (10) of [1] where only a vertical grid is considered. Furthermore,

$$\hat{Z}_{m(A)} = Z_{0(A)} + \frac{j\omega\mu_{(0)}}{2D_x}\sum_{q=-\infty}^{\infty}\left\{\frac{e^{-\Gamma_{mq(0)}b}}{\Gamma_{mq(0)}} \times [{}_{\perp}n^2_{mqz(0)}(1 + {}_{\perp}\Re^{e}_{mq(0)+}) + {}_{||}n^2_{mqz(0)}(1 + {}_{||}\Re^{e}_{mq(0)+})]\right\} \tag{8}$$

Eq. (8) looks identical to (11) in [1] except that the Bessel term is replaced by the exponential because of the use of thin wires instead of the narrow strips in [1]. Using Kummer's convergence methodology [2],[5], (8) is re-expressed as

$$\hat{Z}_{m(A)} = Z_{0(A)} + \frac{j\omega\mu_{(0)}}{2D_x}\left\{(1 - r^2_{mz(0)})\frac{D_xW_A}{\pi} + (1 - r^2_{mz(0)})\Delta^{(iso)}_m + \left({}_{\perp}\Re^{(\infty)}_{(0)+} - r^2_{mz(0)}\,{}_{||}\Re^{(\infty)}_{(0)+}\right)\frac{D_xW_A}{\pi} + \left({}_{\perp}\Delta^{(\infty)}_m + {}_{||}\Delta^{(\infty)}_m\right) + \frac{e^{-\Gamma_{m0(0)}b}}{\Gamma_{m0(0)}} \times \left[1 - r^2_{mz(0)} + {}_{\perp}n^2_{m0z(0)}\,{}_{\perp}\Re^{e}_{m0(0)+} + {}_{||}n^2_{m0z(0)}\,{}_{||}\Re^{e}_{m0(0)+}\right]\right\} \tag{9}$$

Equation (9) looks the same as (21) of [1] except for the presence of the exponential term (the W, $\Delta^{(iso)}_m$ and ${}_{\perp,||}\Delta^{(\infty)}_m$ expressions are also different as shown below) because of the use of thin wires instead of the narrow strips in [1]. A similar expression for $\hat{Z}_{q(B)}$ is obtained by replacing in (9) D_x, A, (A), m, $mz(0)$, $m0z(0)$, $m0(0)$ with D_z, B, (B), q, $qx(0)$, $0qx(0)$, $0q(0)$, respectively. In (9), ${}_{||,\perp}\Re^{(\infty)}_{(0)+}$ is defined in (16)-(17) of

[1] and $\Delta_m^{(iso)}$ by (14) of [6]. Furthermore,

$$W_A = -\ln[1-e^{-(2\pi b/D_x)}] \tag{10}$$

$$\perp\Delta_m^{(\infty)} = \sum_{q=-\infty}^{\infty}{}' \left(\frac{e^{-\Gamma_{mq(0)}b}}{\Gamma_{mq(0)}} \perp n_{mqz(0)}^2 \perp\Re_{mq(0)+}^{e} - \perp\Re_{(0)+}^{(\infty)} \frac{e^{-\frac{2\pi|q|}{D_x}b}}{\frac{2\pi|q|}{D_x}} \right) \tag{11}$$

$$\parallel\Delta_m^{(\infty)} = \sum_{q=-\infty}^{\infty}{}' \left(\frac{e^{-\Gamma_{mq(0)}b}}{\Gamma_{mq(0)}} \parallel n_{mqz(0)}^2 \parallel\Re_{mq(0)+}^{e} + r_{mz(0)}^2 \parallel\Re_{(0)+}^{(\infty)} \frac{e^{-\frac{2\pi|q|}{D_x}b}}{\frac{2\pi|q|}{D_x}} \right) \tag{12}$$

$\hat{Z}_{q(B)}$ is a function of W_B, $\Delta_q^{(iso)}$, $\parallel\Delta_q^{(\infty)}$ which are obtained from (10)-(12) by replacing m, q, D_x, $mqz(0)$, $mz(0)$ with q, m, D_z, $mqx(0)$, $qx(0)$, respectively. $\perp\Delta_q^{(\infty)}$ is given by (14) of [6]. The expressions for U_m and V_q are given by (26)-(27) of [6]. However, the terms in (26) and (27) of [6] are as defined above. Unlike in [6], the convergence of the summations in (26) of [6] is improved here using the aforementioned Kummer's convergence methodology,

$$\sum_{q=-\infty}^{\infty} C_{q(B)}^{(m)} j\frac{(1-\delta_{0q})}{2\pi q} = \frac{\eta_0 r_{mz(0)}}{2D_z\pi}(1+\parallel\Re_{(0)+}^{(\infty)})\ln[1-e^{-(2\pi b/D_x)}]$$
$$+ \sum_{q=-\infty}^{\infty}{}' \left(C_{q(B)}^{(m)} \frac{j}{2\pi q} + \frac{\eta_0 r_{mz(0)}}{4D_z\pi|q|}(1+\parallel\Re_{(0)+}^{(\infty)}) e^{-\frac{2\pi|q|}{D_x}b} \right) \tag{13}$$

and by using eq. (3) of section 1.441 of [13], for $m \neq 0$,

$$\sum_{n=-\infty}^{\infty}{}' Z_{n(A)} j\frac{(1-\delta_{(m-n)0})}{2\pi(m-n)} = j\frac{\mathcal{Z}_{v(A)}}{2\pi m D_z}$$
$$\times\left\{(-1)^m\left[\cos\left(m\pi l/D_z\right)-\mathrm{sinc}\left(m\pi l/D_z\right)\right]-1\right\} \tag{14}$$

For $m = 0$, the series of (14) is equal to zero. The corresponding expressions for the summations in (27) of [6] are obtained from (13) and (14) by replacing the indices/subscripts/superscripts q, m, x, z, A, B, $0q$, $mz(0)$ with m, q, z, x, B, A, $m0$, $qx(0)$, respectively.

The unknown coefficients $_{\vartheta}A'_m$ and $_{\vartheta}B'_q$ in (4)-(5) are computed by solving, a $(2Q+1)\times(2Q+1)$ matrix equation obtained from (28) of [6] and (4)-(5), assuming a maximum harmonic order $\pm Q$. From these coefficients, the values of A_0 and B_0, required in the numerical example that follows, can be obtained from (23) of [6].

III. Numerical Results

To numerically test the proposed Wait-Hill MoM formulation, an example is considered in which the lumped element is a capacitor of value $C = 0.5$ pF, hence $\mathcal{Z}_{v(A)} = \mathcal{Z}_{v(B)} = (j\omega C)^{-1}$, and length $l = 0.5$ mm. The wire radius is $b = 0.06$ mm. The periods are $D_x = D_z = 30$ mm. The substrate consists of two layers. Medium 1 has relative permittivity $\varepsilon_{r(1)} = 4$, relative permeability $\mu_{r(1)} = 4$, conductivity $\sigma_{(1)} = 0.05$ S/m and thickness $b_1 - b_0 = 3$ mm. For medium 2, $\varepsilon_{r(2)} = 2$, $\mu_{r(2)} = 1$, $\sigma_{(2)} = 0.2$ S/m and $b_2 - b_1 = 2$ mm. Media 0 and 3 are assumed to be free space. The incident plane wave amplitude is $E_0 = 1$ V/m. $Q = 8$, hence the matrix size is only 17×17. The series of the coefficients of (4)-(5) have limits $\pm 5Q$. In our i3 PC, the CPU time of our Wait-Hill MoM Matlab code is 0.6 s (approximately) per frequency point and polarization. For the example considered, the transmission coefficient magnitude and phase results are shown in Fig. 2. There is a good agreement between our results and those of CST for both polarizations. The disagreement between the cross-polarized transmission coefficient phase results occurs when the magnitude value of the Wait-Hill MoM coefficient is very small. The CST logfile indicates that our i3 PC takes 279 s / 303 s to compute perpendicular / parallel polarization data, such as those of Fig. 2, using 28128 / 27129 tetrahedrons. It has to be noted that in the CST simulation input and output ports are specified at a distance of 20 mm from the mesh and scattering parameter results are obtained. Hence, for convenience when comparing results, the transmission coefficient, $T_{\varpi\vartheta}$, of the propagating fundamental harmonic is defined here as the ratio of the transmitted electric field at $\mathbf{R}_{out} = \mathbf{R}(x, y_{obs}, z)$ over the incident electric field at $\mathbf{R}_{in} = \mathbf{R}(x, -y_{obs}, z)$, $y_{obs} = 20$ mm where $T_{\varpi\vartheta}$ is

$$T_{\varpi\vartheta} = {}_{\varpi}t_{tot}\frac{E_0\delta_{\varpi\vartheta} - F_{\varpi\vartheta}}{E_0} e^{-j2k_{r(0)}s_{y(0)}y_{obs}} \tag{15}$$

with $F_{\varpi\vartheta} = [{}_{\vartheta}A_0\ {}_{\varpi}n_{00z(0)}/D_x + {}_{\vartheta}B_0\ {}_{\varpi}n_{00x(0)}/D_z]\ \eta_{(0)}/(2s_{y(0)})$ and ${}_{\varpi}t_{tot}$ defined in (28) of [1]. The symbols $\vartheta = \perp, \parallel$ and $\varpi = \perp, \parallel$ represent the incident and transmitted wave polarization, respectively, and $\delta_{\varpi\vartheta}$ is the Kronecker delta.

For the case of an electrically dense mesh, one can assume that A_0, B_0 and Δ are the only unknowns, as was suggested in [4]. Solving the matrix equation, assuming $D_x = D_z = D$ and $\mathcal{Z}_{v(A)} = \mathcal{Z}_{v(B)} = \mathcal{Z}_v$, leads to the following simple analytical expression for the transmission coefficient of (15),

$$T_{\vartheta\vartheta} = {}_{\vartheta}t_{tot}\left(1 - \frac{{}_{\vartheta}\eta(1+{}_{\vartheta}\Re_{00(0)+}^{e})/2}{{}_{\vartheta}\mathcal{Z}_g + {}_{\vartheta}\eta(1+{}_{\vartheta}\Re_{00(0)+}^{e})/2}\right) e^{-j2k_{r(0)}s_{y(0)}y_{obs}} \tag{16}$$

For $\vartheta = \perp$, $_{\perp}\eta = \eta_0 / s_{y(0)}$ and

$$\perp\mathcal{Z}_g = \mathcal{Z}_v - \frac{j\omega\mu_0 D}{2\pi}\perp Q_{(0)}\ln(1-e^{-2\pi b/D}). \tag{17}$$

For $\vartheta = \parallel$, $_{\parallel}\eta = \eta_0\, s_{y(0)}$ and

$$\parallel\mathcal{Z}_g = \mathcal{Z}_v - \frac{j\omega\mu_0 D}{2\pi}\left[\perp Q_{(0)} - \frac{1-s_{y(0)}^2}{2}\parallel Q_{(0)}\right]\ln(1-e^{-2\pi b/D}) \tag{18}$$

with $s_{y(0)} = \cos\xi$, $\perp Q_{(0)} = 1+\perp\Re_{(0)+}^{(\infty)}$ and $\parallel Q_{(0)} = 1+\parallel\Re_{(0)+}^{(\infty)}$. Furthermore, for the cross-polarized transmission coefficients, $T_{\parallel\perp} = T_{\perp\parallel} = 0$. Expressions (17) and (18) correspond to the perpendicular and parallel polarization equivalent circuit impedances, respectively. Expression (16), which includes (17-18), is novel as it evaluates the transmission coefficient of a lumped-element loaded mesh on a stratified substrate consisting of uniform isotropic materials with ε_r, μ_r and σ. No such formula is shown in the related work of [4], [14]. For an

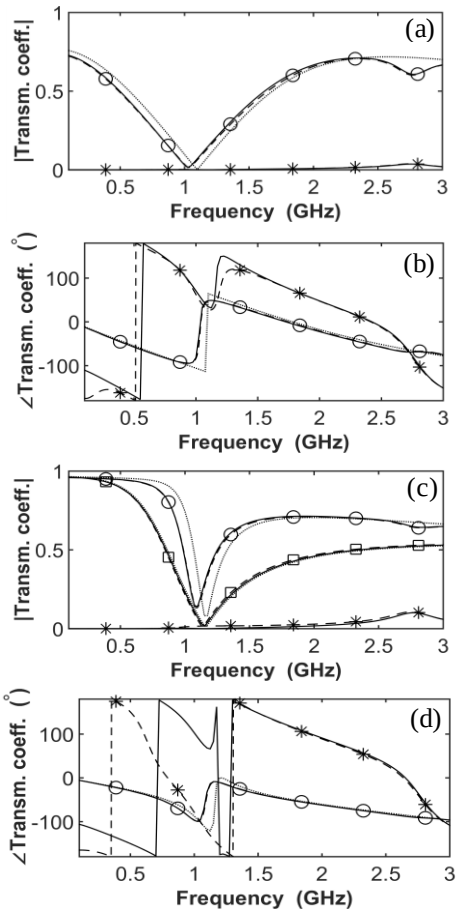

Fig. 2. Transmission coefficient versus frequency for $D_x = D_z = 30$ mm and $C = 0.5$ pF.; (a,c) magnitude and (b,d) phase. Perpendicular polarization (a,b). Parallel polarization (c,d). $\xi = 70°$, $\psi = 22.5°$. CST: dashed line with symbols; co-polarized (○) and cross-polarized (∗) results. Wait-Hill MoM: solid line. Simple analytical expression results: dotted line. In (c), the square symbol (□) results are for $D_x = D_z = 10$ mm and $C = 2$ pF.

unloaded lossy mesh with dielectric materials ($\mu_r = 1$) on either side, that may be different, (17-18) reduce to the impedances derived in [4], eqs. 5.67a-b in [4], if $\mathcal{Z}_v$ is replaced with $Z_w D$ where Z_w is defined by (2) of [5]. If $w << D$, (17-18) simplify to eqs. (5-6) in [14] for an unloaded and lossless mesh, if it is assumed that one of the two regions is free space and the other is a dielectric material ($\mu_r = 1$).

Results from the simple analytical expression (16) are also shown in Fig. 2. The difference between the Wait-Hill MoM results and the analytical results of (16) can be made smaller by reducing the mesh size with respect to the wavelength. As an illustration, the example's period is reduced to $D_x = D_z = 10$ mm (and C is increased to 2 pF to maintain the resonance frequency at around 1 GHz). Fig. 2c shows that the parallel polarization magnitude results of (16) agree well with those of the Wait-Hill MoM ($Q = 5$) and the CST. A good agreement is also observed for the phase and the perpendicular polarization results (not shown in Fig. 2 for clarity).

A Wait-Hill MoM approach can also be used to derive a simple, closed-form expression for the admittance of an electrically dense, lumped element loaded, orthogonal slot array at a general isotropic media interface. Future work will focus on obtaining from sub-domain periodic method of moments, such as the method in [12] that employs roof-top basis functions, the analytical insight presented. Although the approximate kernel thin wire formulation [12] can produce good results, as shown here, it has its well-described solution issues (see references [8] and [9] in [1]) and requires that a thin wire (with radius much smaller than the period) is employed. Hence, we are currently working on extending the VanKoughnett-Buttler approach for the vertical grid of loaded narrow strips in [1] to an orthogonal grid of loaded narrow strips.

IV. Conclusion

A novel entire-domain MoM formulation for modeling plane wave scattering from a lumped-element periodically loaded mesh with a multi-layer substrate was presented. Results, obtained using the Wait-Hill sawtooth function to minimize the number of unknown current harmonic amplitudes and hence computation time, were shown to agree well with those of a commercial software. Finally, for an electrically dense mesh, a novel simple equivalent circuit expression for the transmission coefficient was presented.

References

[1] C. Mias, and A. Freni, "Entire-domain basis function MoM formulation for a substrate backed periodically loaded array of narrow strips," *IEEE Trans. Antennas Propag.*, vol. 63, no. 5, pp. 23251-2331, May 2015.

[2] D.A. Hill, and J.R. Wait, "Electromagnetic scattering of an arbitrary plane-wave by a wire mesh with bonded junctions," *Canadian Journal of Physics*, vol. 54, no. 4, pp. 353-361, 1976.

[3] K.F. Casey, "Electromagnetic shielding behavior of wire-mesh screens," *IEEE Trans. Eleoctromagn. Compat.*, vol. 30, no. 3, pp. 298-306, Aug. 1988.

[4] K.F. Casey, "Electromagnetic shielding by advanced composite materials," Air Force Weapons Laboratory, Interaction Notes, C.E. Baum, Ed. Note 341, June 1977.

[5] J.R. Wait, "On the theory of scattering from a periodically loaded wire grid," *IEEE Trans. Antennas Propagat.*, vol. 25, no. 3, pp. 409-413, May 1977.

[6] C. Mias, and A. Freni, "Generalized Wait-Hill formulation analysis of lumped-element periodically-loaded orthogonal wire grid generic frequency selective surfaces," *Progress in Electromagnetics Research*, vol. 143, pp. 47-66, 2013.

[7] C. Butler, "The equivalent radius of a narrow conducting strip," *IEEE Trans. Antennas Propag.*, vol. 30, no. 4, pp. 755-758, July 1982.

[8] M. Raspopoulos, and S. Stavrou, "Frequency selective surfaces on building materials – air gap impact," *Electron. Lett.*, vol. 43, no. 13, pp. 700-702, June 2007.

[9] J. Hirai, and I. Yokota, "Electromagnetic shielding glass of frequency selective surfaces", in *International Symposium on Electromagnetic Compatibility*, 17-21 May 1999, Tokyo, pp. 314 – 316.

[10] F. Fitzek, R.H. Rashofer, and E.M Biebl, "Broadband matching of high-permittivity coatings with frequency selective surfaces," *Proceedings of the 6th German Microwave Conference (GeMIC)*, 14–16 March 2011, Darmstadt, Germany.

[11] M. Raspopoulos, and S. Stavrou, "Frequency Selective Buildings Through Frequency Selective Surfaces," *IEEE Trans. Antennas Propag.*, vol. 59, no. 8, pp. 2998-3005, Aug. 2011.

[12] B.A. Munk, Frequency Selective Surfaces: Theory and design, John Wiley and Sons, 2000.

[13] I. S. Gradshteyn and I. M. Ryzhik, Table of Integrals, Series, and Products, 7th ed. San Diego, CA: Academic, 2007.

[14] O. Luukkonen, C. Simovski, G. Granet, G. Goussetis, D. Lioubtchenko, A.V. Raisanen, and. S.A. Tretyakov, "Simple and Accurate Analytical Model of Planar Grids and High-Impedance Surfaces Comprising Metal Strips or Patches," *IEEE Trans. Antennas Propag.*, vol. 56, no. 6, pp. 1624-1632, 2008.